search Council of Canada (G.J.S.) for financial support; Ministry of Foreign Affairs, France, for a Lavoisier Fellowship (H.P.M.); and C.N.R.S. Laboratoire des Agrégats Moléculaires et Matériaux Inorganiques, Montpellier, France, for granting a leave of absence to H.P.M.

Supplementary Material Available: Tables of anisotropic thermal parameters (Table 1) and hydrogen atomic coordinates (Table 2) (2 pages); tabulation of calculated and observed structure factor amplitudes (Table 3) (13 pages). Ordering information is given on any current masthead page.

Thermodynamics and Kinetics of Carbon Dioxide Binding to Two Stereoisomers of a Cobalt(I) Macrocycle in Aqueous Solution

Carol Creutz,* Harold A. Schwarz,* James F. Wishart, Etsuko Fujita, and Norman Sutin

Contribution from the Chemistry Department, Brookhaven National Laboratory, Upton, New York 11973. *Received October 1, 1991*

Abstract: The thermodynamics and kinetics of binding of CO_2, CO, and H^+ to *N*-racemic and *N*-meso stereoisomers of the cobalt(I) macrocycle CoL^+ (L = 5,7,7,12,14,14-hexamethyl-1,4,8,11-tetraazacyclotetradeca-4,11-diene) have been determined in aqueous media with use of the pulse radiolysis technique and transient ultraviolet–visible spectroscopy. *N-rac*- or *N-meso*-CoL^+ was produced by the hydrated electron reduction of *N-rac*- or *N-meso*-CoL^{2+}, with *tert*-butyl alcohol generally added to scavenge hydroxyl radicals. Reactions of both *N-rac*- and *N-meso* CoL^+ are readily followed by the disappearance of intense (ϵ 1 × 10^4 M^{-1} cm^{-1}) absorption bands at 630 and 635 nm, respectively. The product absorptions are much less intense (ϵ 200–500 M^{-1} cm^{-1}) and shifted to higher energy (400–500 nm). Carbon dioxide adducts were also produced via the reactions of *N-rac*- or *N-meso*-CoL^{2+} with formate radical $^{\bullet}CO_2^-$ in solutions containing sodium formate and CO_2 and hydrogen ion adducts (hydrides) by the reactions with $^{\bullet}H$ atom in acid solution. The known stereochemistry of the methyl radical additions to *N-rac*- and *N-meso*-CoL^{2+} was used to assign the different isomers of the adducts. Thus, reaction of $^{\bullet}H$ and $^{\bullet}CO_2^-$ with *N-rac*-CoL^{2+} yields *sec-N-rac*-$CoL(H)^{2+}$ and *sec-N-rac*-$CoL(CO_2)^+$, respectively, and the reaction of *N-rac*-CoL^+ with H^+ and CO_2 yields *prim-N-rac*-$CoL(H)^{2+}$ and *prim-N-rac*-$CoL(CO_2)^+$, respectively. As expected, only *N*-meso adducts are obtained from either *N-meso*-CoL^+ or *N-meso*-CoL^{2+}. Formation constants for the complexes (determined by analysis of equilibrium absorptions or equilibration kinetics) at 25 °C are $CoL(CO_2)^+$, 2.5 × 10^8 M^{-1} (prim-*N*-rac), 6.0 × 10^6 M^{-1} (*N*-meso); $CoL(CO)^+$, 1.6 × 10^8 M^{-1} (prim-*N*-rac), 0.8 × 10^8 M^{-1} (*N*-meso); $CoL(H)^{2+}$, 2.5 × 10^{11} M^{-1} (prim-*N*-rac), ≥7.9 × 10^{13} M^{-1} (*N*-meso). The rate constants are large and generally parallel the stablity of the adduct. The following are values of k (M^{-1} s^{-1}) for addition at 25 °C: CO_2, 1.7 × 10^8 (prim-*N*-rac), 1.5 × 10^7 (*N*-meso); CO, 5.0 × 10^8 (prim-*N*-rac), 8.3 × 10^8 (*N*-meso); H^+, 3.0 × 10^9 (prim-*N*-rac), 2.3 × 10^9 (*N*-meso).

Introduction

Cobalt complexes have attracted attention as potential catalysts for photo- and electroreduction of water to H_2 and of carbon dioxide to CO and HCO_2^-.[1-5] The cobalt(I) complexes, which are accessible through photo- or electroinduced one-electron reduction of the cobalt(II) complexes, may bind hydrogen ion or carbon dioxide and, in some cases, facilitate their reduction. A particularly attractive family for systematic studies is the tetraazacyclotetradecyl macrocycle series,[6] in which the cobalt(II)/(I) potential ranges from −0.34 to −1.65 V (versus SCE) in acetonitrile.[7] In such a series, the relationships between metal reduction potentials, ligand steric factors, etc. and the reactivity of the complex toward both the binding and reduction of small molecules may be explored. Indeed, this problem is currently being studied by several groups.[7-10]

Of the above series, the macrocycle L = 5,7,7,12,14,14-$(CH_3)_6$-1,4,8,11-tetraazacyclotetradeca-4,11-diene has received the most intensive study to date. For this ligand, the Co(III)/(II) and Co(II)/(I) reduction potentials are ca. −0.2 and −1.34 V, respectively, vs SCE in acetonitrile.[7] The cobalt(III) complexes are six-coordinate, the low-spin d^7 cobalt(II) complexes appear to be five- or six-coordinate, and the low-spin d^8 cobalt(I) complexes are four- or five-coordinate.[11,12] Stereoisomers of the complexes arise through the chirality of the saturated nitrogen atoms.[13] Although *cis*-Co(III)LB (B = bidentate ligand) is known, most complexes of this series are trans, with the four nitrogen atoms of the macrocycle occupying the equatorial plane of the complex. At minimum, two trans isomers (*N*-meso and *N*-racemic) are possible. In aqueous solutions of the five- or

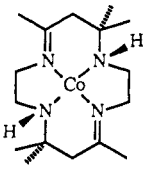

N-rac L

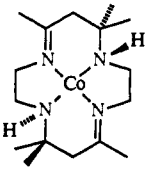

N-meso L

six-coordinate CoL^{2+} (the coordination sphere of the cobalt(II) being completed by solvent molecule(s)), the *N*-rac isomer is favored at equilibrium but the *N*-meso isomer can also be studied in pH <7 solutions.[12] The low-spin d^8 CoL^+ can also exist as either isomer, as will be seen. When the axial positions of the complex are asymmetrically substituted (CoLXY, X and Y different ligands), three isomers are possible—*N*-meso, primary *N*-rac, and

(1) Brown, G. M.; Brunschwig, B. S.; Creutz, C.; Endicott, J. F.; Sutin, N. *J. Am. Chem. Soc.* **1979**, *101*, 1298-1300.
(2) Fisher, B.; Eisenberg, R. *J. Am. Chem. Soc.* **1980**, *102*, 7363-7366.
(3) Pearce, D. J.; Pletcher, D. *J. Electroanal. Chem.* **1986**, *197*, 317.
(4) Simpson, T. C.; Durand, R. R. *Electrochim. Acta* **1988**, *33*, 581.
(5) Tinnemans, A. H. A.; Koster, T. P. M.; Thewissen, D. M. W. H.; Mackor, A. **1984**, *103*, 288.
(6) Tait, A. M.; Lovecchio, F. V.; Busch, D. H. *Inorg. Chem.* **1977**, *16*, 2206.
(7) Fujita, E.; Creutz, C.; Sutin, N.; Szalda, D. J. *J. Am. Chem. Soc.* **1991**, *113*, 343-353.
(8) Gangi, D. A.; Durand, R. R. *Chem. Soc., Chem. Commun.* **1986**, 697.
(9) Creutz, C.; Schwarz, H. A.; Wishart, J. F.; Fujita, E.; Sutin, N. *J. Am. Chem. Soc.* **1989**, *111*, 1153-4.
(10) Schmidt, M. H.; Miskelly, G. M.; Lewis, N. S. *J. Am. Chem. Soc.* **1990**, *112*, 3420-3426.
(11) Szalda, D. J.; Fujita, E.; Creutz, C. *Inorg. Chem.* **1989**, *28*, 1446-50.
(12) Szalda, D. J.; Schwarz, C. L.; Endicott, J. F.; Fujita, E.; Creutz, C. *Inorg. Chem.* **1989**, *28*, 3214-19.
(13) Warner, L. G.; Rose, N. J.; Busch, D. H. *J. Am. Chem. Soc.* **1968**, *90*, 6938-6946.

0002-7863/91/1513-3361$02.50/0

secondary *N*-rac. Here, secondary ("sec") and primary ("prim") refer, respectively, to the face on which the axial 7,14-CH_3 and 1,8-NH groups are found.

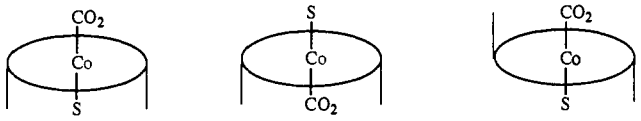

In early work, Vasilevskis and Olson[14] characterized the cobalt(I) complex formed upon electroreduction of *N-meso*-CoL^{2+} in acetonitrile. Tait, Hoffman, and Hayon[15] subsequently used pulse-radiolytic methods to study electron- and proton-transfer reactions of CoL^+, generated from *N-rac*-CoL^{2+}, in water. We have been characterizing the interaction of CoL^+ with CO_2[7,9,16] and recently gave a preliminary account of our pulse radiolytic studies with the *N*-rac isomer in water.[9] Here, we present a full report of that work and the results of our work with the *N*-meso isomer, as well. As will be seen, although this isomerism sometimes poses practical problems in identifying the isomeric nature of reactants and products, it does afford an opportunity for exploring the role of steric effects on both the kinetics and thermodynamics of ligand binding.

Experimental Section

The perchlorate salts of the *N-rac*-[17] and *N-meso*-CoL^{2+}[18] complexes were prepared and characterized[12] by literature methods. [*Warning*: The perchlorate salts used in this study may be explosive and potentially hazardous.] The CO_2/N_2 gas mixtures were obtained from MG Industries and their compositions ascertained by gas chromatography (they were mislabeled). Solutions were deaerated by bubbling with Ar, CO, N_2O, or CO_2, depending upon the experiment. The weighed cobalt samples were always added to deaerated solutions.

Pulse radiolysis was performed by using 40–200-ns pulses of electrons from a 2-MeV van de Graaff accelerator. The samples were thermostated, and the optical path length was generally 6.1 cm. Between 5×10^{-8} and 1×10^{-5} M radicals were produced per pulse.

When CO_2 solutions were used, "carbonic acid" equilibria and the solubility of CO_2 (0.033 M at 1 atm and 25 °C) had to be taken into account;[19] $NaHCO_3$ solutions were generally added to adjust the pH (above pH 5). Otherwise, H_2SO_4, NaOH, or phosphate, acetate, or borate buffers were added to adjust the pH. The radical species present shortly after the pulse were determined by the relative concentrations of the various reagents. For example, for studies of formate radical reactions, 0.1 M HCO_2^- was used to convert the primary product •OH to $•CO_2^-$ and CO_2 (in concentration 20–100 times Co(II)) was used to convert e^-_{aq} to $•CO_2^-$. In other experiments, *tert*-butyl alcohol (0.5 M) served as •OH radical scavenger, while e^-_{aq} reduced either CO_2 or CoL^{2+}.

Results

Both *N*-meso and *N*-rac isomers were studied here, with the conditions under which they could be studied being dictated by the stabilities of the cobalt(II) complexes. *N-rac*-CoL^{2+} is the more stable isomer in water, and the isomerization of the *N-meso* isomer is hydroxide ion catalyzed.[12] Thus, experiments with the latter were limited to pH <7 for practical reasons. As will be seen, the CoL^+ species retain the conformation of the parent CoL^{2+} species for the course of the experiment (sometimes 10 s), except possibly at high pH.

The cobalt(I) complexes were produced by pulse radiolysis of aqueous solutions containing the cobalt(II) complexes and sodium formate or alcohols. Ninety percent of the radicals produced in water radiolysis are about equally divided between e^-_{aq} and •OH. The remaining 10% are •H atoms (some H_2 and H_2O_2 are also formed). Table I summarizes literature rate constants for radical processes relevant to this study.

Table 1. Literature Values (25 °C) for Rate Constants Used in This Study

reaction	k, M^{-1} s^{-1}	ref
$e^-_{aq} + CO_2 \rightarrow •CO_2^-$	7.7×10^9	*a*
$e^-_{aq} + N_2O \rightarrow •OH + N_2 + OH^-$	9.1×10^9	*a*
$e^-_{aq} + H^+ \rightarrow •H$	2.3×10^{10}	*a*
$•OH + HCO_2^- \rightarrow H_2O + •CO_2^-$	3.2×10^9	*a*
$•OH + HCO_2H \rightarrow H_2O + •CO_2^- + H^+$	1.3×10^8	*a*
$•OH + (CH_3)_3COH \rightarrow H_2O + (•CH_2)(CH_3)_2COH$	6.0×10^8	*a*
$•OH + (CH_3)_2C(H)OH \rightarrow H_2O + (OH)(CH_3)_2C•$ (86%) $\rightarrow H_2O + (•CH_2)(CH_3)C(H)OH$ (13%)	1.9×10^9	*a*
$•OH + (CH_3)_2SO \rightarrow •CH_3 + (CH_3)S(O)OH$	6.6×10^9	*a*
$•H + HCO_2^- \rightarrow H_2 + •CO_2^-$	2.1×10^8	*a*
$•H + (CH_3)_3COH \rightarrow H_2 + (•CH_2)(CH_3)_2COH$	1.7×10^5	*a*
$•H + (CH_3)_2C(H)OH \rightarrow H_2O + (OH)(CH_3)_2C•$	7.4×10^7	*a*
$•H + •H \rightarrow H_2$	1.0×10^{10}	*a*
$•CO_2^- + •CO_2^- \rightarrow C_2O_4^{2-}$	0.4×10^9	*b*
$2(•CH_2)(CH_3)_2COH \rightarrow$	0.7×10^9	*b*
$2(OH)(CH_3)_2C• \rightarrow (CH_3)_2CO + (CH_3)_2C(H)OH$	0.6×10^9	*b*

[a] Buxton, G. V.; Greenstock, C. L.; Hellman, W. P.; Ross, A. B. *J. Phys. Chem. Ref. Data* **1988**, *17*, 513. [b] Ross, A. B.; Neta, P. *Natl. Bur. Stand. Ref. Ser. NSRDS-NBS* **1982**, 70.

•OH Scavengers. Since CoL^{2+} reacts very rapidly[15] with the •OH radical, the addition of •OH scavengers was essential and it was necessary to know the fates of the radicals produced from the scavengers. When N_2O-saturated (0.025 M) *tert*-butyl alcohol (0.5 M) was used, both e^-_{aq} (which reacts with N_2O to give •OH) and •OH were converted to the *tert*-butyl alcohol radical $(CH_3)_2(CH_2•)C(OH)$ and the interaction of Co(II) (0.05–1.8 mM) with the radical could be studied. Reaction of this radical with the *N*-rac isomer was observed only at very high $[CoL^{2+}]$ ($k = 1.4 \times 10^6$ M^{-1} s^{-1}), and the spectrum of the adduct was not determined. The radical was found to add more rapidly to *N-meso*-CoL^{2+} ($k = 2 \times 10^7$ M^{-1} s^{-1}) and produced a species (presumably the alkyl complex) with an absorption maximum at ~490 nm ($\epsilon \sim 150$ M^{-1} cm^{-1}). This adduct appeared to be a "permanent" product, and no evidence for its reaction with Co(I) or its adducts was found. The *tert*-butyl alcohol radical reacts with both CoL^+ and $CoL(H)^{2+}$ (see below).

In a few experiments at high pH, 2-propanol served as an •OH scavenger. Under such conditions (0.1 M 2-propanol, pH >11), the deprotonated radical $(CH_3)_2CO^-$ is a strong reducing agent ($E° = -2.0$ V[20]) and reduces *N-rac*-CoL^{2+} to CoL^+ ($k = 3.5 \times 10^8$ M^{-1} s^{-1}).

With formate ion, the third •OH scavenger used here, $•CO_2^-$ formate radical is produced. Formate radical can also be produced from the reaction of CO_2 with e^-_{aq} (see Table I). In 0.1 M $NaHCO_2$ saturated with CO_2, both CoL^{2+} isomers react very rapidly with $•CO_2^-$. Reaction of the *N*-rac isomer with $•CO_2^-$ ($k = 8.5 \times 10^8$ M^{-1} s^{-1}) yields ≥95% addition at 25 °C. At 66 °C, however, 20–30% CoL^+ is produced, in addition to the formate radical adduct. Reaction of the *N*-meso isomer with $•CO_2^-$ at 25 °C ($k = 3 \times 10^9$ M^{-1} s^{-1}) results in ca. 80% addition, with ca. 20% of the reaction yielding Co(I). The properties of these adducts are described later in the context of CO_2 adducts.

Reactions of CoL^{2+} with $•CH_3$. The methyl radical adducts of CoL^{2+} are known species[21–26] and were produced here for comparison purposes. The reaction of *N-rac*-CoL^{2+} (0.7 mM) with $•CH_3$ radical was studied at pH 7 (1 mM phosphate buffer) in N_2O-saturated 0.01 M aqueous $(CH_3)_2SO$. The rate constant for addition was 6×10^7 M^{-1} s^{-1} at 25 °C (and about 1×10^8

(14) Vasilevskis, J.; Olson, D. C. *Inorg. Chem.* **1971**, *10*, 1228.
(15) (a) Tait, A. M.; Hoffman, M. Z.; Hayon, E. *J. Am. Chem. Soc.* **1976**, *98*, 86. (b) Tait, A. M.; Hoffman, M. Z.; Hayon, E. *Int. J. Radiat. Phys. Chem.* **1976**, *8*, 691.
(16) Fujita, E.; Szalda, D. J.; Creutz, C.; Sutin, N. *J. Am. Chem. Soc.* **1988**, *110*, 4870–1.
(17) Goedken, V. L.; Kildahl, N. K.; Busch, D. H. *J. Coord. Chem.* **1977**, *7*, 89.
(18) Rillema, D. P.; Endicott, J. F.; Papaconstantinou, E. *Inorg. Chem.* **1971**, *10*, 1739.
(19) (a) Palmer, D. R.; van Eldik, R. *Chem. Rev.* **1983**, *83*, 651–731. (b) Butler, N. N. *Carbon Dioxide Equilibria and Their Applications*; Addison-Wesley: Reading, MA, 1982.
(20) Schwarz, H. A.; Dodson, R. W. *J. Phys. Chem.* **1989**, *93*, 409.
(21) Roche, T. S.; Endicott, J. F. *J. Am. Chem. Soc.* **1972**, *94*, 8622.
(22) Roche, T. S.; Endicott, J. F. *Inorg. Chem.* **1974**, *13*, 1575.
(23) Heeg, M. J.; Endicott, J. F.; Glick, M. D. *Inorg. Chem.* **1981**, *20*, 1196.
(24) (a) Bakac, A.; Espenson, J. H. *Inorg. Chem.* **1989**, *28*, 4319. (b) Lee, S.; Espenson, J. H.; Bakac, A. *Inorg. Chem.* **1990**, *29*, 3442–3447.
(25) Endicott, J. F.; Kumar, K.; Schwarz, C. L.; Perkovic, M. W.; Lin, W.-K. *J. Am. Chem. Soc.* **1989**, *111*, 7411.
(26) Szalda, D. J.; Schwarz, C. L.; Creutz, C. *Inorg. Chem.* **1991**, *30*, 586–588.

Table II. Comparison of Cobalt(II) Rate Constants at 25 °C

reaction	k(*N*-rac), M^{-1} s^{-1}	k(*N*-meso), M^{-1} s^{-1}
$(^{\bullet}CH_2)(CH_3)_2COH + CoL^{2+} \rightarrow CoL((CH_2)(CH_3)_2COH)^{2+}$	1.4×10^6	2×10^7
$(CH_3)_2CO^- + CoL^{2+} \rightarrow CoL^+$	3.5×10^8	
$^{\bullet}CH_3 + CoL^{2+} \rightarrow CoL(CH_3)^{2+}$	0.6×10^8	2.3×10^8
$CoL^{2+} + e^-_{aq} \rightarrow CoL^+$	4.4×10^{10}	4.7×10^{10}
$H^{\bullet} + CoL^{2+} \rightarrow CoL(H)^{2+}$	1.1×10^9	1.3×10^9
$^{\bullet}CO_2^- + CoL^{2+} \rightarrow CoL(CO_2)^+$	8.5×10^8 (>95%)	3×10^9 (80%)
$^{\bullet}CO_2^- + CoL^{2+} \rightarrow CoL^+$	(<5%)	(20%)

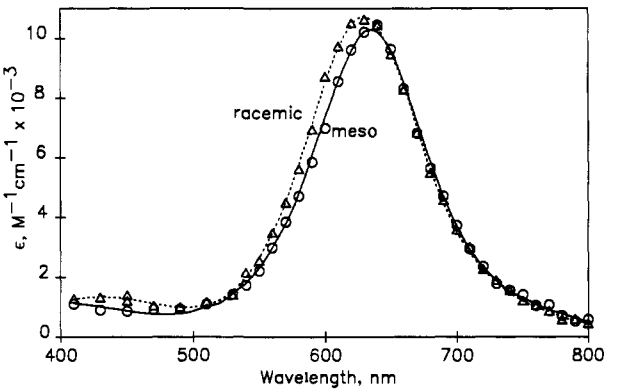

Figure 1. Electronic absorption difference spectra of *N-rac-* and *N-meso*-CoL^+ formed from the reaction of CoL^{2+} (0.4 mM) with e^-_{aq} in 0.5 M *tert*-butyl alcohol containing 0.1 mM phosphate buffer (pH ~7) at 25 °C.

M^{-1} s^{-1} at 63 °C). The corrected absorption spectrum of the adduct (λ_{max} 460 nm, ϵ 190 M^{-1} cm^{-1}; sh 380 nm, ϵ 300 M^{-1} cm^{-1}) is in good agreement with that reported[25,26] for *sec-N-rac*-$CoL(CH_3)(H_2O)^{2+}$. Methyl radical addition to *N-meso*-CoL^{2+} is faster[24a] (2.3×10^8 M^{-1} s^{-1}) and yields[21,22] *N-meso*-$CoL(CH_3)(H_2O)^{2+}$.

Rate constants for the CoL^{2+} reactions are given in Table II.

Cobalt(I) Complexes. Both *N-rac*-[15] and *N-meso*-CoL^{2+} react rapidly with e^-_{aq} to produce intensely absorbing CoL^+ products (eq 1). The rate constant for reduction of *N*-rac-CoL^{2+} is[15] 4.4×10^{10} M^{-1} s^{-1} and we find 4.7×10^{10} M^{-1} s^{-1} for *N-meso*-CoL^{2+}.

$$CoL^{2+} + e^-_{aq} \rightarrow CoL^+ \qquad (1)$$

The absorption spectra of the two isomers are very similar (Figure 1), but there are reproducible differences between them, notably the greater width of the 630-nm band and the presence of the ca. 450-nm band for the *N*-rac isomer.

The lifetimes of the CoL^+ species are limited by first-order reactions with water. We find that the rate constants for these processes are 2.3×10^3 s^{-1} for *N-rac*-CoL^+, in agreement with the literature,[15] and 1.8×10^4 s^{-1} for *N-meso*-CoL^+. These rate constants were measured in the presence of 0.5 M *tert*-butyl alcohol, and the reaction of *tert*-butyl alcohol radical with *N-rac*-CoL^+ was manifested as an increase in the cobalt(I) disappearance rate with increasing radical concentration [R•]: $k_{obsd} = 2.3 \times 10^3 + 2 \times 10^8$[R•] s^{-1}. Some of the radical decayed by recombination so that the rate constant for the reaction of R• with *N-rac*-CoL^+ is larger than 2×10^8 M^{-1} s^{-1} but likely in the range $(2-3) \times 10^8$ M^{-1} s^{-1}.

Protonation of Cobalt(I). Three protonated cobalt(I) species ($CoL(H)^{2+}$) were characterized in this study. Both CoL^+ isomers react rapidly with acids by a pathway first-order in cobalt(I) and HA concentrations. The products are the prim-*N*-rac (eq 2R) and *N*-meso (eq 2M) hydride complexes. Kinetic data for the

$$N\text{-}rac\text{-}CoL^+ + HA \rightarrow prim\text{-}N\text{-}rac\text{-}CoL(H)^{2+} + A^- \qquad (2R)$$

$$N\text{-}meso\text{-}CoL^+ + HA \rightarrow N\text{-}meso\text{-}CoL(H)^{2+} + A^- \qquad (2M)$$

protonation reactions, obtained in argon-saturated 0.5 M *tert*-butyl alcohol solutions, are presented in Table III, and corrected spectra

Table III. Rate Constants for Protonation of CoL^+ by Acids (HA) at 25 °C

			k, M^{-1} s^{-1}		
			N-rac-CoL^+		
HA	pK_A	I, M	this work	lit.[a]	*N-meso*-CoL^+
H_3O^+	−1.75	0.015		3.1×10^9	2.3×10^9
HCOOH	3.5	0.02	1.7×10^8		1.8×10^8
CH_3COOH	4.5	0.1	1.1×10^8	0.75×10^8	0.8×10^8
$H_2PO_4^-$	6.5	0.1	0.8×10^8	0.98×10^8	1.2×10^8
		0.008	1.2×10^8		
HCO_3^-	10.3	0.1	2.5×10^6		
H_3BO_3	9.3	0.1	0.7×10^5		
HPO_4^{2-}	12.25	0.2		1×10^5	

[a] Tait, A. M.; Hoffman, M. Z.; Hayon, E. *J. Am. Chem. Soc.* **1976**, *98*, 86.

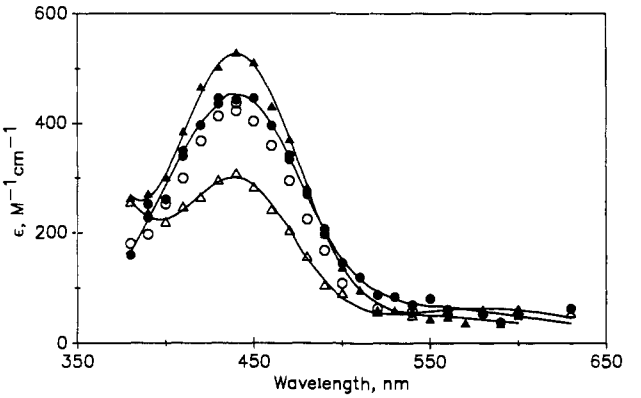

Figure 2. Corrected spectra of (solid triangles) *prim-N-rac*-$CoL(H)^{2+}$ from reaction of *N-rac*-CoL^+ with $H_2PO_4^-$, (solid circles) *N-meso*-$CoL(H)^{2+}$ from reaction of *N-meso*-CoL^+ with $H_2PO_4^-$, (open circles) *N-meso*-$CoL(H)^{2+}$ from reaction of *N-meso*-CoL^{2+} with H atoms, (open triangles) *sec-N-rac*-$CoL(H)^{2+}$ from reaction of *N-rac*-CoL^{2+} with H atoms. The experimentally determined difference spectra have been corrected for the appropriate CoL^{2+} absorption changes. All solutions contained 0.4 mM CoL^{2+} and 0.5 M *tert*-butyl alcohol. The reactions with $H_2PO_4^-$ were carried out at pH 7 and those with H atoms in 0.3 M H_2SO_4.

of the products are shown in Figure 2. The spectrum of the product derived from the *N*-rac isomer is independent of temperature in the range 10–60 °C.

Hydrides can also be formed by reaction of hydrogen atoms with CoL^{2+}. Spectra obtained in 0.5 M *tert*-butyl alcohol solutions containing 0.3 M H_2SO_4 (to convert all e^-_{aq} to •H atoms) are also shown in Figure 2. It is seen that the same spectrum (*N-meso*-$CoL(H)^{2+}$) is observed whether *N-meso*-CoL^+ reacts with acids (eq 2M) or H• atoms react with *N-meso*-$Co(L)^{2+}$ (eq 3M). The

$$H^{\bullet} + N\text{-}meso\text{-}CoL^{2+} \rightarrow N\text{-}meso\text{-}CoL(H)^{2+} \qquad (3M)$$

spectra obtained when *N-rac*-CoL^+ reacts with acids is not the same as that obtained when H• atoms react with *N-rac*-CoL^{2+}. In light of the formation[26] of the *sec*-methyl complex from the reaction of methyl radical and *N-rac*-CoL^{2+}, it is reasonable to suggest that the latter spectrum is that of *sec-N-rac*-$CoL(H)^{2+}$. The rate constants found were 1.3×10^9 M^{-1} s^{-1} for reaction 3M and 1.1×10^9 M^{-1} s^{-1} for reaction 3R.

$$H^{\bullet} + N\text{-}rac\text{-}CoL^{2+} \rightarrow sec\text{-}N\text{-}rac\text{-}CoL(H)^{2+} \qquad (3R)$$

With boric acid = HA in eqs 2R and 2M, the product 440-nm absorption was ca. 30% smaller than with HA = H_3O^+ or $H_2PO_4^-$, possibly suggesting parallel formation of both *prim-*, and *sec-N-rac*-$CoL(H)^{2+}$ isomers.

The pK_a of *prim-N-rac*-$CoL(H)^{2+}$ can be measured in basic solutions. Sufficient acid ($H_2PO_4^-$ in this case) must be present to suppress the relative importance of the first-order CoL^+ decay. Thus, concentrated solutions must be used, and the equilibrium can be studied only at the lower pH edge of the "titration" curve. Fortunately, the CoL^+ spectrum is intense (ϵ 1×10^4 M^{-1} cm^{-1}),

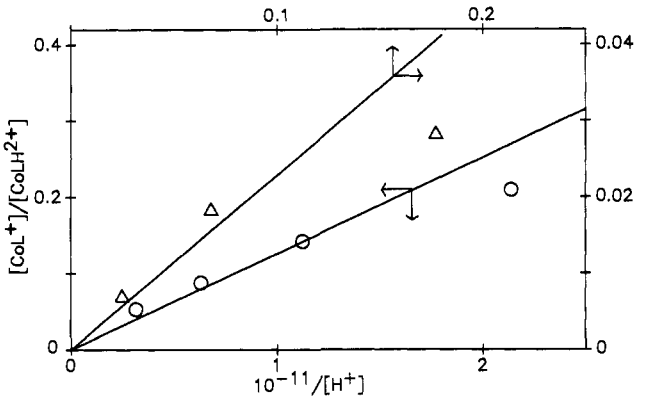

Figure 3. Determination of the pK_a of *sec-N-rac*-CoL(H)$^{2+}$ in the presence of (open triangles) 0.1 M phosphate, top and right scales, and (open circles) 0.5 M phosphate, bottom and left scales. All solutions contained 0.4 mM *N-rac*-CoL^{2+} and 0.5 M *tert*-butyl alcohol. The pH was varied with NaOH. The ordinate is calculated from the 630-nm absorbance of CoL$^+$ remaining after the equilibration.

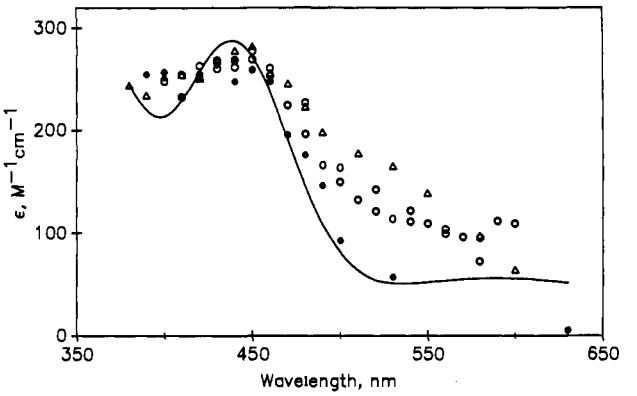

Figure 4. Corrected spectra observed following the first-order decay of CoL$^+$ in water at 25 °C: (open circles) from *N-rac*-CoL$^+$ at the end of the 2.3 × 10^3 s^{-1} decay, (open triangles) from *N-meso*-CoL$^+$ at the end of the 1.8 × 10^4 s^{-1} decay (both solutions contained 0.5 M *tert*-butyl alcohol), and (filled circles) from *N-rac*-CoL$^+$ at the end of 1.6 s^{-1} (decarboxylation step) in solutions containing 0.1 M sodium formate. The solid curve is the spectrum of *sec-N-rac*-CoL(H)$^{2+}$ from Figure 2.

and the hydride absorption is negligible at 630 nm. Thus, the pK_a can be estimated from data obtained when as little as 2% of the conjugate base CoL$^+$ remains at equilibrium. The pK_a's were calculated from the relation $\epsilon_{obsd}/(\epsilon_{Co(I)} - \epsilon_{obsd}) = K/[H^+]$. From the data (shown in Figure 3), pK_a values of 11.8 and 11.6 are obtained fro 0.5 and 0.1 M phosphate media, respectively, at 25 °C. The ionic strengths of these solutions (1.5 and 0.3 M) are higher than those used in our other experiments (typically 0.1 M).

It was not possible to determine the pK_a of *N-meso*-CoL(H)$^{2+}$ by this method because *N-meso*-CoL^{2+} is not stable in alkaline solution.

The formation of *prim-N-rac*-CoL(H)$^{2+}$ from reaction of *N-rac*-CoL$^+$ with $H_2PO_4^{2-}$ in the presence of 0.5 M *tert*-butyl alcohol is followed by a slow partial decay of the hydride at 600–1500 s^{-1}, depending upon initial concentrations. This decrease is due to the reaction of the *tert*-butyl alcohol radical R$^\bullet$ with the hydride:

$$R^\bullet + \textit{prim-N-rac}\text{-CoL(H)}^{2+} \rightarrow RH + \textit{N-rac}\text{-CoL}^{2+}$$

Absorbances before and after the reaction indicate that only about 18% of the R$^\bullet$ reacts in this fashion after a single pulse, which means that the rate constant is smaller than for the R$^\bullet$ recombination (Table I). However, since much of the remaining CoL(H)$^{2+}$ accumulates from pulse to pulse and R$^\bullet$ does not, after many pulses a larger fraction of R$^\bullet$ reacts in this manner (40–50% after four pulses). The rate observed for hydride disappearance is heavily influenced by the second-order R$^\bullet$ recombination, and the fraction of the hydride surviving at subsequent pulses is not well determined, but taking the latter fraction as 50% and dividing the observed rate constant by the estimated concentration of hydride, the rate constant for the hydrogen atom abstraction is 2 × 10^8 M^{-1} s^{-1}, with an uncertainty of about 50%.

First-Order Decays of CoL$^+$. As noted earlier, in the absence of added acids (and other potential reactants such as CO_2), the CoL$^+$ absorptions decay by first-order processes with rate constants of 1.8 × 10^4 s^{-1} and 2.3 × 10^3 s^{-1} at 25 °C for the *N*-meso and *N*-rac isomers, respectively. The spectra of the products of these reactions are shown in Figure 4. It can be seen that the spectra are very similar to one another and are possibly the same. Also shown in Figure 4 is the spectrum of *sec-N-rac*-CoL(H)$^{2+}$ (the closest match from Figure 2). The latter is similar to the other two but definitely not identical with them. These spectra were obtained in solutions containing 0.5 M *tert*-butyl alcohol, and the behavior of the solutions at long times was complicated by the reactions of the *tert*-butyl alcohol radical. To eliminate this complication, the *tert*-butyl alcohol was replaced by formate ion and studies of the *N-rac*-CoL$^+$ system were extended to longer times. In the formate media, *N-rac*-CoL$^+$ formed, as well as a CoL(CO$_2$)$^+$ species discussed later. The CoL(CO$_2$)$^+$ product decays slowly (1.6 s^{-1}) by loss of CO_2 to yield CoL$^+$. Thus, in

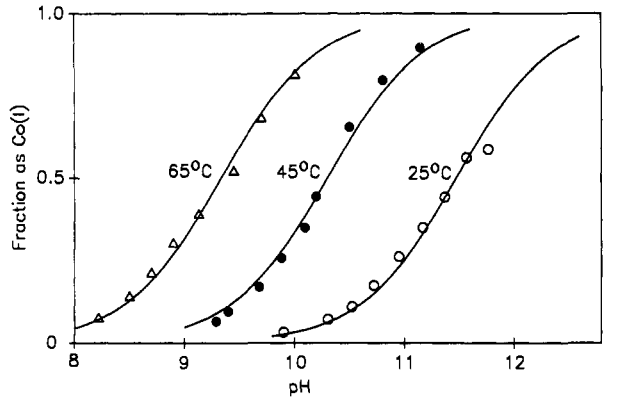

Figure 5. Determination of the pK_a of *sec-N-rac*-CoL(H)$^{2+}$ where the fraction as Co(I) is the ratio of the equilibrium absorbance of *N-rac*-CoL$^+$ at the end of the faster of two steps to the initial absorbance measured at 630 nm. The solid curves are calculated for pK_a's of 11.5, 10.3, and 9.3 at 25, 45, and 65 °C. Solutions contained 0.5 mM *N-rac*-CoL^{2+}, 0.5 M *tert*-butyl alcohol, and 2 mM borate buffer.

0.1 M formate solutions of *N-rac*-CoL^{2+} at pH 9 (1.2 mM borate buffer), all radicals eventually produce CoL$^+$, which reacts with water, so the spectrum of the product of the latter reaction can be studied at long times. The spectrum obtained at long times in formate media is also shown in Figure 4, and it may be seen that it is much closer to that of *sec-N-rac*-CoL(H)$^{2+}$. From these comparisons, we propose that reaction of *N-rac*-CoL$^+$ with water yields two species (*sec-N-rac*-CoL(H)$^{2+}$ and a species absorbing near 500 nm). The *sec-N-rac*-CoL(H)$^{2+}$ is the more stable of the two, and the 500-nm absorbing species converts to *sec-N-rac*-CoL(H)$^{2+}$ at long times.

The involvement of water in the reaction is suggested by the relatively long lifetime of CoL$^+$ in nonaqueous solvents[7,14,16] and by the pH dependence of the phenomenon. Again, only *N-rac*-CoL^{2+} could be studied. NaOH was used to vary the pH of solutions containing 0.5 M *tert*-butyl alcohol and 1 mM borate. The decay of the CoL$^+$ was monitored at 630 nm and was found to be complex. At pH 11.6, for example, when the absorbance was monitored for about 5 ms, it first dropped to about 60% of its initial value with the rate constant of 4.7 × 10^3 s^{-1} but then decreased further with a rate constant of ca. 0.6 × 10^3 s^{-1}. The absorbance at the end of the faster stage increases with pH and gives a pK of 11.5 at 25 °C for *N-rac*-CoL$^+$ (third curve in Figure 5). The rate constant for this step increased with pH in agreement with the pK of 11.5. In contrast, the rate constant for the slower stage did not change significantly with pH and depended on the time scale over which the data were collected. The dependence on the time scale probed indicates that at least one other process

must be taking place. Since these data were obtained in *tert*-butyl alcohol solutions, one complication is the reaction of *tert*-butyl alcohol radical with both CoL^+ and $CoL(H)^{2+}$ (both rate constants are 2×10^8 M^{-1} s^{-1}). With the 6×10^{-7} M initial radical concentration, these parallel *tert*-butanol radical reactions contribute a ca 1000-s^{-1} component to the observed decay and result in some loss of cobalt(I) and hydride complexes. However, this may not be the only source of kinetic complexity.

The kinetics can be discussed in terms of the following equations

$$N\text{-}rac\text{-}CoL^+ + H_2O \rightleftharpoons sec\text{-}N\text{-}rac\text{-}CoL(H)^{2+} + OH^- \quad (4R)$$

$$N\text{-}rac\text{-}CoL^+ + H_2O \rightleftharpoons X_{500} + OH^- \quad (4'R)$$

$$N\text{-}rac\text{-}CoL^+ + H_2O \underset{\text{(slow)}}{\rightleftharpoons} N\text{-}meso\text{-}CoL(H)^{2+} + OH^- \quad (4''R)$$

where X_{500} is the species absorbing at 500 nm (to be discussed later). Thus, the fastest step would be the establishment of a kinetic steady state between CoL^+ and the products of reactions 4R and 4'R. The next slower step would be the equilibration of X_{500} with *sec*-*N*-*rac*-$CoL(H)^{2+}$ (via CoL^+). However, the rates of these two steps (4R and 4'R) are not sufficiently different to allow their resolution from the data. The fact that the data in Figure 5 give a reasonably good fit to a single pK, together with the fact that the 500-nm species is less stable than *sec*-*N*-*rac*-$CoL(H)^{2+}$ (discussed earlier), gives some confidence that the observed pK_a values are close to those of *sec*-*N*-*rac*-$CoL(H)^{2+}$. Thus, the parameters that may be calculated from the curves in Figure 5 are assigned to *sec*-*N*-*rac*-$CoL(H)^{2+}$ and are the following: pK_a's of 11.5 at 25 °C, 10.3 at 45 °C, and 9.3 at 65 °C. These give $K_{4R} = 2.9 \times 10^{-2}$ M at 25 °C, 8.0×10^{-3} M at 45 °C, and 2.8×10^{-3} M at 65 °C; $\Delta H°(4R) = -11$ kcal mol^{-1}, and $\Delta S°(4R) = -50$ cal mol^{-1} K^{-1}. The entropy change is reasonable for the production of a doubly charged species in the reaction. It should be clear, however, that even though the curves in Figure 5 appear to be reasonably precise the ambiguities in the kinetic undoubtedly introduce fairly large systematic errors. The ambiguity is compounded by the fact that the cobalt(I) absorption completely dominates the spectrum.

The identification of the product of the slow step as *N*-*meso*-$CoL(H)^{2+}$ (eq 4''R) is tentative. This step was studied further at higher pH with 0.1 M 2-propanol as scavenger in the presence of 1 mM cobalt(II) and 0.004–0.08 M NaOH. At such high pH, the 2-propanol radical is deprotonated and quantitatively reduces cobalt(II) to cobalt(I). With 0.08 M NaOH (pH 12.7), the CoL^+ decayed at 660 s^{-1} and the product spectrum agreed well with that of *N*-*meso*-$CoL(H)^{2+}$, with about 6% of the CoL^+ spectrum mixed in (mainly evident at the 630-nm peak). If this [CoL^+] is assumed to be the equilibrium level, then a pK_a of 13.9 is calculated for *N*-*meso*-$CoL(H)^{2+}$. Unfortunately, our data are not sufficient to clarify the nature of the mechanism of the equilibration (eq 4''R).

Stabilities of CoL^+ Isomers. The relative stability of the two CoL^+ isomers was probed with *N*-*rac*-CoL^{2+}/*N*-*meso*-CoL^{2+} mixtures. It was assumed that, with total CoL^{2+} concentration of about 2 mM, the outer-sphere electron-transfer equilibrium (eq 5) is established rapidly compared to the CoL^+ disappearance

$$N\text{-}meso\text{-}CoL^+ + N\text{-}rac\text{-}CoL^{2+} \rightleftharpoons N\text{-}meso\text{-}CoL^{2+} + N\text{-}rac\text{-}CoL^+ \quad (5)$$

rate (by reactions 4M and 4R, among others). In this case, the decay of the CoL^+ absorption should remain first-order but should depend on the ratio of the isomers

$$k_{obsd} = k_R(1 - f_M) + k_M f_M$$

where k_R and k_M are the two first-order rate constants and f_M is the equilibrium fraction of CoL^+ present as the *N*-meso isomer. The experiments were carried out with 0.2–1.8 mM CoL^{2+}, 0.5 M *tert*-butyl alcohol, and pH 7 solutions, the pH being maintained with 20 mM phosphate buffer. The ratio [*N*-*rac*-CoL^{2+}]/[*N*-*meso*-CoL^{2+}] was varied from 0.5 to 4. The Co(I) disappearance kinetics were exponential, and the best fit to the equations gave $k_R = 4.2 \times 10^3$ s^{-1}, $k_M = 1.7 \times 10^4$ s^{-1}, and $K_5 = 0.8 \pm 0.4$. The value of k_R is considerably larger than 2.3×10^3 s^{-1} ($k_{4R} + k_{4'R}$),

$$f_M = 1/(1 + K_5[N\text{-}rac\text{-}CoL^{2+}]/[N\text{-}meso\text{-}CoL^{2+}])$$

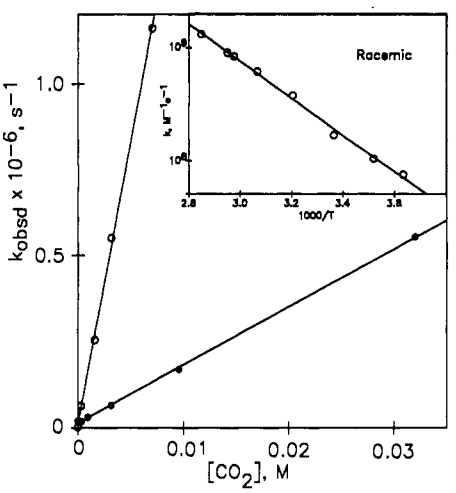

Figure 6. Pseudo-first-order rate constant for the reaction of CoL^+ with CO_2 as a function of the CO_2 concentration at 25 °C in the presence of 0.5 M *tert*-butyl alcohol and 1 mM CoL^{2+}: (open circles) *N*-*rac*-CoL^+, (filled circles) *N*-*meso*-CoL^+. The inset shows the temperature dependence of the *N*-rac rate constant (k_{10R}).

$$N\text{-}meso\text{-}CoL^{2+} \rightleftharpoons N\text{-}rac\text{-}CoL^{2+} \quad (6)$$

$$N\text{-}meso\text{-}CoL^+ \rightleftharpoons N\text{-}rac\text{-}CoL^+ \quad (7)$$

mainly because the pH had to be kept low (6.7) with about 2×10^{-5} M phosphate buffer so that reaction 2R contributed about 2.0×10^3 s^{-1} to the rate. Since[12] $K_6 \geq 10$, it is concluded that $K_7 \geq 10$. The fact that the racemic isomer of CoL^+ is the more stable means that the pK_a of 13.9 for *N*-*meso*-$CoL(H)^{2+}$ reported above really applies to the reaction

$$N\text{-}meso\text{-}CoL(H)^{2+} \rightleftharpoons N\text{-}rac\text{-}CoL^+ + H^+ \quad (8)$$

and combining K_8 and K_{4R} gives $K_9 = 200$. Thus, these experiments suggest that the *N*-meso hydride is favored at equilibrium. Finally, we note that, while the kinetics of eq 5 were not observed directly, the other observations require that $k_5 \geq 1 \times 10^7$ M^{-1} s^{-1}.

$$N\text{-}rac\text{-}CoL(H)^{2+} \rightleftharpoons N\text{-}meso\text{-}CoL(H)^{2+} \quad (9)$$

Reactions with CO_2 and CO. The kinetics of the addition of CO_2 to CoL^+ were determined at 630 nm with solutions 0.5 M in *tert*-butyl alcohol and 0.4–1 mM in CoL^{2+} saturated with 1–100% CO_2. For the *N*-rac isomer, the solution pH ranged from 6 to 3.5, depending upon the CO_2 level; experiments with the *N*-meso isomer were carried out at pH 5.8, while the pH being adjusted by the addition of $NaHCO_3$ solution. The measured pseudo-first-order rate constants were corrected for small contributions from eqs 2 (HA = H^+, HCO_3^-) and 4. The CO_2 dependence of the corrected k_{obsd} values at 25 °C is shown in Figure 6. The second-order rate constants for eq 10 are 1.7×10^8 and 1.6×10^7 M^{-1} s^{-1} for *N*-rac and *N*-meso isomers, respectively, at 25 °C. The temperature dependence of the rate constant for the *N*-rac isomer (Figure 6) yields $\Delta H^‡ = 6.9$ kcal mol^{-1} and $\Delta S^‡ = 2.5$ cal K^{-1} mol^{-1}.

$$CoL^+ + CO_2 \xrightarrow{k_{10}} CoL(CO_2)^+ \quad (10)$$

The rate constants for addition of carbon monoxide to CoL^+ (eq 11) at 25 °C in the presence of 0.5 M *tert*-butyl alcohol saturated with CO (9.5×10^{-4} M) were found to be 5.0×10^8 M^{-1} s^{-1} (*N*-rac) and 8×10^8 M^{-1} s^{-1} (*N*-meso).

$$CoL^+ + CO \xrightarrow{k_{11}} CoL(CO)^+ \quad (11)$$

The absorption spectra of the various CO_2 adducts are compared in Figure 7. The product of $^•CO_2^-$ addition to *N*-*rac*-CoL^{2+} (eq

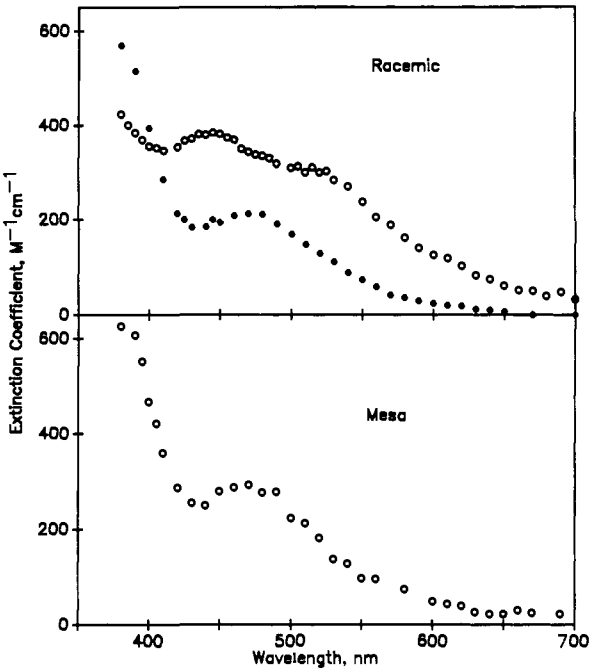

Figure 7. Corrected absorption spectra for $CoL(CO_2)^+$ species. The upper curves are for (open circles) *prim-N-rac*-$CoL(CO_2)^+$ from reaction of *N-rac*-CoL^+ with CO_2 in the presence of 0.5 M *tert*-butyl alcohol and for (filled circles) *sec-N-rac*-$CoL(CO_2)^+$ from reaction of *N-rac*-CoL^{2+} with $^{\bullet}CO_2^-$ in CO_2-saturated 0.1 M formate solutions. The lower curve is for *N-meso*-$CoL(CO_2)^+$ from reaction of $^{\bullet}CO_2^-$ with *N-meso*-CoL^{2+}. The reaction of *N-meso*-CoL^+ with CO_2 is too slow for quantitative production of the product.

12R) is not the same as that of CO_2 addition to *N-rac*-CoL^+,[9] and by analogy with the results for methyl radical addition the products are assigned as *sec-N-rac*-$CoL(CO_2)^+$ and *prim-N-rac*-$CoL(CO_2)^+$, respectively. The spectrum of the *N-meso*-CoL^+

$$^{\bullet}CO_2^- + \textit{N-rac}\text{-}CoL^{2+} \rightarrow \textit{sec-N-rac}\text{-}CoL(CO_2)^+ \quad (12R)$$

$$CO_2 + \textit{N-rac}\text{-}CoL^+ \rightarrow \textit{prim-N-rac}\text{-}CoL(CO_2)^+ \quad (10R)$$

carbon dioxide addition product was not measured: The reaction is relatively slow, and *N-meso*-CoL^{2+} disappearance by eq 4M is so rapid that high $[CO_2]$ is required. However, at high $[CO_2]$, most of the CO_2 adduct is produced via the formate radical path (eq 12M). (However, as noted above, only 80% of the $^{\bullet}CO_2^-$ + *N-meso*-CoL^{2+} reaction results in addition; the remainder yields $CoL^+ + CO_2$.)

$$^{\bullet}CO_2^- + \textit{N-meso}\text{-}CoL^{2+} \rightarrow \textit{N-meso}\text{-}CoL(CO_2)^+ \quad (12M)$$

$$CO_2 + \textit{N-meso}\text{-}CoL^+ \rightarrow \textit{N-meso}\text{-}CoL(CO_2)^+ \quad (10M)$$

As is shown in Figure 8, the spectrum of *prim-N-rac*-$CoL(CO_2)^+$ is temperature-dependent, with λ_{max} 440 nm at 0 °C and 520 and 60 °C. Taking as extinction coefficients ϵ_{520} 10 M^{-1} cm^{-1} for the low-temperature (yellow) form and 900 M^{-1} cm^{-1} for the high-temperature (purple) form, the equilibrium constant for eq 13 was evaluated as a function of temperature, and the values

$$\underset{\text{purple}}{\textit{prim-N-rac}\text{-}CoL(CO_2)^+} \rightleftharpoons \underset{\text{yellow}}{\textit{prim-N-rac}\text{-}CoL(CO_2)^+} \quad (13)$$

$K_{13}(298) = 2.0$, $\Delta H^\circ_{13} = -6.1$ kcal mol^{-1} and $\Delta S^\circ_{13} = -19$ cal K^{-1} mol^{-1} were obtained. The ϵ_{520} value of 900 M^{-1} cm^{-1} for the high-temperature form was taken from the value determined in acetonitrile.[7,16] The best value, based on the pulse radiolysis data alone, is 1100 M^{-1} cm^{-1}, which would lead to a smaller ΔH°_{13} (−5.4 kcal mol^{-1}); however, the fit is not significantly worse when ϵ_{520} 900 is used. The extinction coefficients were corrected for production of hydride (2% at 2 °C to 16% at 68 °C) before calculating the equilibria. The spectra of the pure forms were calculated from the equilibrium constants and the full spectra at the three temperatures in Figure 8.

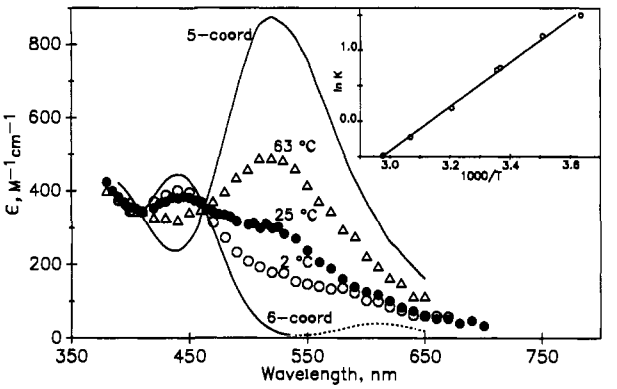

Figure 8. Corrected absorption spectrum of *prim-N-rac*-$CoL(CO_2)^+$ as a function of temperature. It is assumed that the high-temperature form is a five-coordinate species and that the low-temperature form is six-coordinate. The temperature dependence of the derived equilibrium constant, based on the assumption that the five-coordinate spectra are the same in water and acetonitrile, is shown in the inset. The derived spectra for the pure five- and six-coordinate forms are also shown (curves). The dotted portion of the spectrum of the six-coordinate species ($\epsilon \sim 30$ M^{-1} cm^{-1}) is suspect, as it lies in the same position as the parent CoL^+ peak (ϵ 1 × 10^4 M^{-1} cm^{-1}).

Equilibrations of CO_2 and CO Complexes. In CO_2 and CO containing solutions, the initial fate of CoL^+ (produced by eq 1) depends upon the relative concentrations of acids HA (eq 2) and CO_2 or CO. Thus, the distribution of species present $\sim 10^{-3}$ s after the electron pulse is kinetically determined. Equilibration of $CoL(CO_2)^+$ or $CoL(CO)^+$ with $CoL(H)^{2+}$ does, however, occur on a longer (0.1–10 s) time scale. Different approaches were used in evaluating the stability constants of the adducts derived from *N-rac*- and *N-meso*-CoL^+. For the *N*-rac complexes, the stabilities of the adducts with respect to *prim-N-rac*-$CoL(H)^{2+}$ (eqs 14R and 15R) were determined[9] by evaluating the optical absorption

$$\textit{prim-N-rac}\text{-}CoL(CO_2)^+ + H^+ \rightleftharpoons \textit{prim-N-rac}\text{-}CoL(H)^{2+} + CO_2 \quad (14R)$$

$$\textit{prim-N-rac}\text{-}CoL(CO)^+ + H^+ \rightleftharpoons \textit{prim-N-rac}\text{-}CoL(H)^{2+} + CO \quad (15R)$$

of the mixtures of $CoL(H)^{2+}$ and $CoL(CO_2)^+$ or $CoL(CO)^+$ at the end of the equilibration step on the 1–10-s time scale as a function of $[H^+]$ and $[CO_2]$ or [CO]. For the *N*-meso isomers, the analogous equilibria lie to far to the right in the limited pH range (≤7) over which *N-meso*-CoL^{2+} is "stable", so equilibrium constants for eqs 10M and 9M were obtained from the ratios of forward and reverse rate constants by measuring the CO_2 (k_{-10M} and CO (k_{-11M}) dissociation rate constants.

***N*-rac Isomer.** As reported previously,[9] K_{14R} = 1100 at 25 °C (0.1 M $NaHCO_2$, pH 3–8, (0.032–3.2) × 10^{-3} M CO_2) and K_{15R} = 970 (0.5 M *tert*-butyl alcohol, 1–10 mM acetate or phosphate buffer, pH 4–8, 0.14 or 1.0 mM CO). We have extended these studies to higher temperatures, and the results are presented in Figure 9. K_{14R} was 5.3 × 10^2 at 50 °C and 1.1 × 10^3 at 25 °C from which $\Delta G^\circ_{14R}(298) = -4.1$ kcal mol^{-1}, $\Delta H^\circ_{14R} = -5.7$ (±1.5) kcal mol^{-1}, and $\Delta S^\circ_{14R} = -5$ (±5) cal K^{-1} mol^{-1} are obtained for the CO_2 complex. For the CO complex, K_{15R} = 3000 at 25 °C and 1250 at 62 °C, from which $\Delta G^\circ_{15R}(298) = -4.7$ kcal mol^{-1}, $\Delta H^\circ_{15R} = -4.8$ (±1.5) kcal mol^{-1}, and $\Delta S^\circ_{15R} = 0$ (±5) cal K^{-1} mol^{-1}. The errors are based on an estimated relative accuracy of 20%. The equilibrium constant for eq 8R can be calculated to be 2.5 × 10^8 M^{-1} from K_{14R} = 1.1 × 10^3 and the pK_a of *prim-N-rac*-$CoL(H)^{2+}$ (estimated as 11.4 at 0.1 M ionic strength).

For these systems, the best equilibrium data were obtained in formate media. However, the equilibration kinetics were more complicated in formate than in *tert*-butyl alcohol media because of the presence of the formate radical adduct *sec-N-rac*-$CoL(CO_2)^+$. The latter undergoes irreversible CO_2 loss ($k \simeq 1.6$ s^{-1} at 25 °C) on roughly the same time scale as the equilibrations

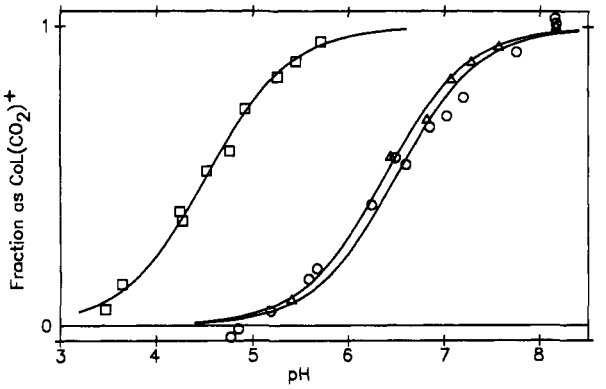

Figure 9. Equilibration of *prim-N-rac*-$CoL(CO_2)^+$ and *prim-N-rac*-$CoL(CO)^+$ with *prim-N-rac*-$CoL(H)^{2+}$ (eq 14 and 15). The equilibrium fraction of *prim-N-rac*-$CoL(CO_2)^+$ or *prim-N-rac*-$CoL(CO)^+$ is plotted as a function of pH. All solutions contained 0.1 M formate and 1 mM phosphate or acetate buffer: (squares) *prim-N-rac*-$CoL(CO_2)^+$ from 0.4 mM *N-rac*-CoL^{2+} and 0.16 mM CO_2 at 50 °C (530 nm), (open circles) *prim-N-rac*-$CoL(CO)^+$ from 0.95 mM CO at 25 °C (390 nm), (open triangles) *prim-N-rac*-$CoL(CO)^+$ from 0.53 mM CO at 62 °C (390 nm).

(eqs 14R and 15R). Thus, the time profiles associated with the equilibrations are not exponential. In *tert*-butyl alcohol solutions, the *tert*-butyl alcohol radical disappears on a time scale (within 1 ms) rapid compared with that for the equilibration reactions, and the equilibration kinetics can then be fit to a single exponential.

The equilibration mechanism[9] involves dissociation of $CoL(CO_2)^+$, $CoL(CO)^+$, and $CoL(H)^{2+}$ to CoL^+. With the steady-state assumption for $[CoL^+]$

$$k_{obsd} = k_{-10}f_2 + k_{-2}[A^-](1 - f_2) \qquad (16)$$

where $f_2 = k_2[HA]/(k_2[HA] + k_{10}[CO_2])$. Of course, if more than one acid is present, $k_2[HA]$ and $k_{-2}[A^-]$ are summed over all. The value of k_{-10} can be calculated from the known values of k_{10} (1.7×10^8 M^{-1} s^{-1}) and K_{10} (4.5×10^8 M^{-1}) to be 0.38 s^{-1}. Similarly, values of k_{-2} can be calculated from the pK_a of *prim-N-rac*-$CoL(H)^{2+}$, the pK_a of the acid HA, and the known values of k_2 (Table II). Thus, the rate of equilibration for eq 14R can be calculated from known values. Of course, the same is true for $CoL(CO)^+$ equilibrations when eq 11 is substituted for eq 10. The rates of CO equilibration in phosphate solutions and the rates of CO_2 equilibrations in phosphate and acetic acid/acetate solutions were followed. The ionic strength varied from 0.01 to 0.15 M in these experiments, and k_2 and k_{-2} are ionic strength dependent. Appropriate values for k_2 and k_{-2} were obtained from $\log_{10}(k/k_0) = 1.02[Z_aZ_bI^{1/2}/(1 + I^{1/2}) - 0.2I]$. In Figure 10, observed and calculated rates of equilibration are compared. The line drawn has unit slope, so it is clear that the observed kinetics strongly support the mechanism in Scheme I.

Scheme I

$$CoL(CO_2)^+ \underset{k_{10}}{\overset{k_{-10}}{\rightleftharpoons}} CoL^+ + CO_2$$

$$CoL^+ + HA \underset{k_{-2}}{\overset{k_2}{\rightleftharpoons}} CoL(H)^{2+} + A^-$$

***N*-meso Isomer.** At long times, both CO_2 and CO adducts of *N-meso*-CoL^+ were found to be converted quantitatively to the hydride complex at pH 7 (eqs 14M and 15M). The error of measurement is about 10%, so the effective K values are greater than 10^8. Thus, with $[CO_2] = 0.033$ M, the limit $K_{14M} \geq 3 \times 10^6$ is obtained, and with $[CO] = 9.5 \times 10^{-4}$ M $K_{15M} \geq 1 \times 10^5$ is implicated. The CO_2 and CO binding constants could, however, be determined from the kinetic behavior of the system. As noted earlier, high nonequilibrium proportions of the CO_2 (eq 12M) or CO (eq 11M) complex can be generated when [HA] is relatively low; the rates of equilibration (formation of $CoL(H)^{2+}$) can then be followed on a longer time scale. The equilibration mechanism is analogous to Scheme I, but k_{-2M} is negligible so that

$$k_{obsd} = k_{-10M}f_2$$

Plots of k_{obsd} vs f_2 are shown in Figure 11. Analysis of these results yields $k_{-10M} = 2.5$ s^{-1} and $k_{-11M} = 10$ s^{-1}. From $K = k_f/k_r$, the equilibrium constants $K_{10M} = 6 \times 10^6$ M^{-1} (CO_2) and $K_{11M} = 8 \times 10^7$ M^{-1} (CO) are obtained at 25 °C. These results also provide an independent estimate of the affinity of *N-meso*-CoL^+ for H^+ (eq 2M). Since $K_{14M} \geq 3 \times 10^6$ and $K_{10M} = 6 \times 10^6$ M^{-1}, then $K_{2M} \geq 1.8 \times 10^{13}$ M^{-1}—that is, pK_a(*N-meso*-$CoL(H)^{2+}$) > 13.3 at 25 °C.

$$N\text{-}meso\text{-}CoL^+ + H^+ \rightarrow N\text{-}meso\text{-}CoL(H)^{2+} \qquad (2M)$$

The rate and equilibrium constants for CoL^+ reactions are summarized in Table IV.

$$N\text{-}meso\text{-}CoL(CO_2)^+ + H^+ \rightleftharpoons N\text{-}meso\text{-}CoL(H)^{2+} + CO_2 \qquad (14M)$$

$$N\text{-}meso\text{-}CoL(CO)^+ + H^+ \rightleftharpoons N\text{-}meso\text{-}CoL(H)^{2+} + CO \qquad (15M)$$

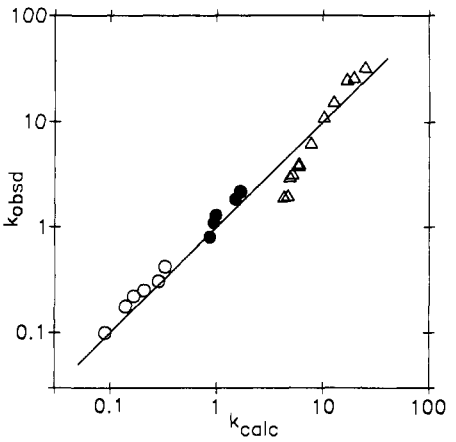

Figure 10. Comparison of observed and calculated rate constants (eq 16) for equilibration of *prim-N-rac*-$CoL(CO_2)^+$ and *prim-N-rac*-$CoL(CO)^+$ with *prim-N-rac*-$CoL(H)^{2+}$ at 25 °C in the presence of 0.5 M *tert*-butyl alcohol: (open circles) CO_2 adduct with varying acetate buffer concentration and varying pH, (filled circles) CO_2 adduct with varying phosphate buffer concentration and varying pH, (triangles) CO adduct with varying phosphate buffer concentration and pH.

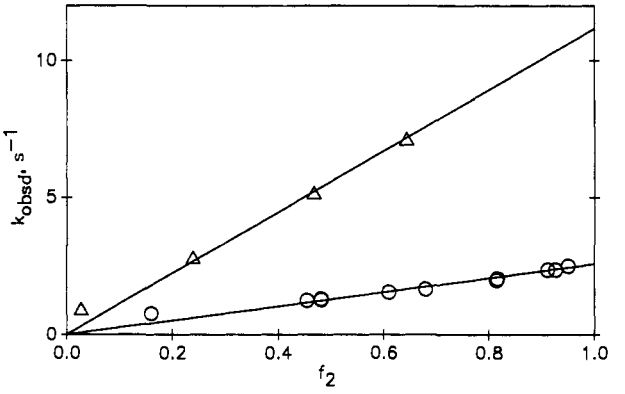

Figure 11. Dependence of rate constants for equilibrations (eqs 14M and 15M) on the fraction of the intermediate *N-meso*-CoL^+, which reacts with acid (principally $H_2PO_4^-$), calculated from eq 16: (circles) CO_2 adduct (eq 14M), (triangles) CO adduct (eq 15). The rate constant for dissociation to CoL^+ is given by the right-hand intercepts at $f_2 = 1$.

Discussion

Nature of the Products. Although the CoL^+ species produced by reaction of *N-rac*- and *N-meso*-CoL^{2+} have very similar visible absorption spectra, the body of evidence amassed in this study shows that there are indeed two CoL^+ isomers and that these retain the configuration of the parent CoL^{2+} complex for at least several seconds unless electron-transfer equilibration pathways (eq 5) are

Table IV. Rate Constants for CoL^+ and $CoL(H)^{2+}$ Reactions at 25 °C[a]

reaction	rate const	*N*-rac	*N*-meso
$CoL^+ + CO_2 \rightleftharpoons CoL(CO_2)^+$	k_f, M^{-1} s^{-1}	1.7×10^8	1.6×10^7
	k_r, s^{-1}	(0.38) (prim)	2.7
	k_r, s^{-1}	1.6 (sec)	
	k_f/k_r, M^{-1}	4.5×10^8 (prim)	(6.0×10^6)
$CoL^+ + CO \rightleftharpoons CoL(CO)^+$	k_f, M^{-1} s^{-1}	5.0×10^8	8.3×10^8
	k_r, s^{-1}	3.1	11
	k_f/k_r, M^{-1}	1.6×10^8	(0.8×10^8)
$CoL^+ + H^+ \rightleftharpoons CoL(H)^{2+}$	k_f, M^{-1} s^{-1}	3.1×10^9[b]	2.4×10^9
	k_r, s^{-1}	1.2×10^{-2} (prim)	$<10^{-4}$
	K, M^{-1}	2.5×10^{11} (prim)	$>8 \times 10^{13}$
	K, M^{-1}	3.2×10^{11} (sec)	
$CoL^+ + N_2O \rightarrow$	k, M^{-1} s^{-1}	2×10^7	1×10^7
$CoL^+ + (^\bullet CH_2)(CH_3)_2COH \rightarrow$	k, M^{-1} s^{-1}	2×10^8	
$CoL(H)^{2+} + {}^\bullet CO_2^- \rightarrow$	k, M^{-1} s^{-1}	6×10^9	
$CoL(H)^{2+} + (^\bullet CH_2)(CH_3)_2COH \rightarrow$	k, M^{-1} s^{-1}	2×10^8	

[a] Values in parentheses are derived from the other tabulated values. [b] Tait, A. M.; Hoffman, M. Z.; Hayon, E. *J. Am. Chem. Soc.* **1976**, *98*, 86.

Table V. Electronic Absorption Spectra as a Function of Isomer[a]

complex	prim-*N*-rac	sec-*N*-rac	*N*-meso
$(CH_3)CoL(H_2O)^{2+}$	468 (300)[b]	462 (192)[c]	470 (228)[b]
$(CH_3)CoL(NCS)^+$	448 (208)[b]	450[c]	458 (273)[b]
$(CO_2)CoL(H_2O)^+$	440 (510)	470 (210)	470 (288)
$(H)CoL(H_2O)^{2+}$	440 (520)	440 (300)	440 (445)

[a] Prim or sec refers to the position of the first ligand listed (i.e., CH_3, CO_2, or H). [b] Roche, T. S.; Endicott, J. F. *Inorg. Chem.* **1974**, *13*, 1575. [c] Endicott, J. F.; Kumar, K.; Schwarz, C. L.; Perkovic, M. W.; Lin, W.-K. *J. Am. Chem. Soc.* **1989**, *111*, 7411.

provided. Their different "natural lifetimes" (eq 4) and their very different reactivities with CO_2 provide striking kinetic evidence for the existence of two CoL^+ isomers. Furthermore, the spectra of the various CO_2 adducts (Figure 9) require that *N-rac*-CoL^+ be produced from *N-rac*-CoL^{2+} and that *N-meso*-CoL^+ be produced from *N-meso*-CoL^{2+}. As outlined in the Introduction, two *N-rac*-$Co(CO_2)$ isomers (primary and secondary) are possible, but there is a single *N-meso*-$Co(CO_2)$ isomer. We found that, when *N-rac*-CoL^{2+} is the starting material, different products result from ${}^\bullet CO_2^-$ addition to CoL^{2+} and from CO_2 addition to CoL^+. We believe that the former is the secondary $CoL(CO_2)^+$ isomer since ${}^\bullet CH_3$ radical addition to *N-rac*-CoL^{2+} gives the secondary CH_3 isomer.[26] Thus, the other isomer, which results from CO_2 addition to CoL^+ in *N*-rac solutions, must be the primary *N*-rac isomer. The latter has spectral features very similar to those of the adduct characterized[7] in nitrile solvents. Furthermore, crystals isolated from concentrated solutions of the latter contain a dimer of the five-coordinate primary isomer.[16] A third CO_2 species is produced by ${}^\bullet CO_2^-$ addition to *N-meso*-CoL^{2+} (and presumably by CO_2 addition to *N-meso*-CoL^+). Evidence of a fourth isomer of the $CoL(CO_2)^+$ complex comes from the temperature dependence of the spectrum of *prim-N-rac*-$CoL(CO_2)^+$ (Figure 9, eq 13) in water[9] and in nitrile[7,16] solvents. As we have already noted,[7,9,16] we believe the low-temperature form to be six-coordinate and the high-temperature form to be five-coordinate.

Apart from the CO adducts, which are five-coordinate, square-planar species,[11] and the high-temperature form of *prim-N-rac*-$CoL(CO_2)^+$, the complexes produced here are believed to be six-coordinate species, with the cobalt coordination sphere completed by a bound water molecule. This model and the isomer assignments given above are supported by the adducts' electronic spectra. In Table V, the visible absorption maxima of the hydride and CO_2 complexes are compared with the lowest ligand-field band observed for the methyl complexes. It can be seen there that the absorption spectra of the hydride and carbon dioxide complexes are related to those of the alkylcobalt(III) complexes. The intensity pattern (prim-*N*-rac > *N*-meso > sec-*N*-rac) observed for the methyl complexes is retained for the CO_2 and hydride complexes, thus supporting the isomer assignments given above. Furthermore, the similarity of the three sets of spectra suggests that these bands should be considered as six-coordinate cobalt(III) ligand-field transitions for the hydride and CO_2 complexes, as well. This analysis has proven useful for the metallocarboxylate[27]

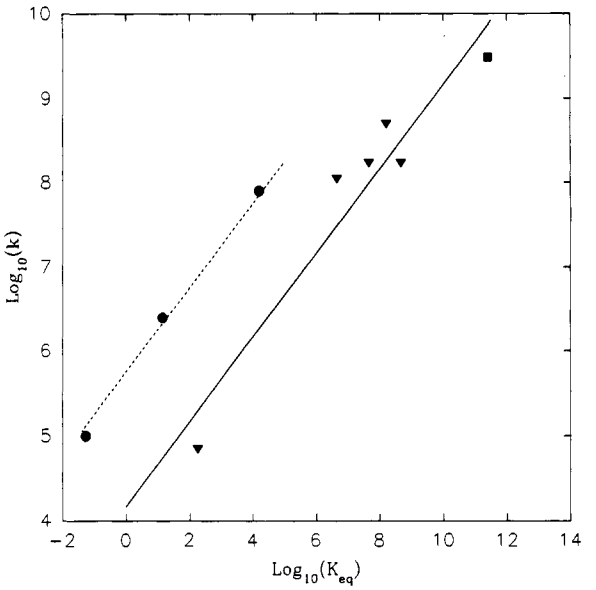

Figure 12. Dependences of rate constants for *N-rac*-CoL^+ reactions with acids, CO_2, and CO on the equilibrium constant for the reaction: (circles) anionic acids, (triangles) neutral reactants, and (square) H_3O^+. The slopes of the lines are 0.5 (data from Tables III and IV).

trans-$Co(en)_2(H_2O)(CO_2R)^{2+}$ as well. For complexes of the latter type, $-CO_2R^-$ (R = H, C_2H_5) were found to be higher field ligands than the cyanide ion. On the basis of data available for complexes of this macrocycle family,[22] the order $H^- \approx CN^- \geq -CO_2^{2-} \geq CH_3^-$ is inferred. It is noteworthy that the ligand-field band positions are not identical for the three isomers of the CH_3 or CO_2 complexes. This probably results from variations of the M–C and M–O bond distances (a result of steric strain), as has been seen for the CH_3 complexes.[22,23,26]

Mechanistic Implications. Cobalt(I) Reactions. The contrasts in the "substitutional" behavior of *N-rac*-CoL^{2+} and *N-rac*-CoL^+ invoked above to account for the differing product distributions from cobalt(II) and cobalt(I) reactions is noteworthy. The behavior of the cobalt(II) complex implicates binding of a water molecule at its primary face (as has been found in crystals of the complex[12]). In contrast, the behavior of the cobalt(I) complex seems to require that the cobalt(I) be simply four-coordinate, square-planar in solution as is observed[7] for *N-meso*-CoL'^+ (L' = 3,5,7,7,10,12,14,14-octamethyl-1,4,8,11-tetraazacyclotetradeca-4,11-diene) in the solid state. Thus, the reactions of CoL^+ with CO_2, CO, and acids are indeed addition reactions. This picture is also consistent with the very large magnitude of the rate constants for the reactions. In a report of earlier pulse radiolysis

(27) Katz, N. E.; Szalda, D. J.; Chou, M. H.; Creutz, C.; Sutin, N. *J. Am. Chem. Soc.* **1989**, *111*, 6591.

studies of *N-rac*-CoL^+, the dependence of protonation rate constants on acid strength was noted.[15] As is illustrated in Figure 12, our data also conform with this trend. Note that the intercept of the plot provides a measure of the "intrinsic" proton-transfer barrier between –OH and Co(I); from the magnitude of the intercept, the rate constant for such a proton transfer at zero driving force is estimated as $k_0 = 10^4$–10^5 M^{-1} s^{-1}. The latter is of interest in comparison with the results of Norton and colleagues for proton transfer between –NH and transition-metal centers[28] ($k_0 \approx 10^5$ M^{-1} s^{-1}) and of Gandler and Bernasconi ($k_0 = 10^2$ M^{-1} s^{-1}) for proton transfer[29] between nitrogen bases and $-CH_3$ in $(CO)_5Cr{=}C(OCH_3)_2$. Figure 12 also reveals another interesting correlation: Rate constants for addition of CO_2 and CO to *N-rac*-CoL^+ fall on the same free energy plot as those for proton transfer from uncharged acids. Furthermore, the slope of the plot is approximately $^1/_2$, as would be expected for an ideal associative reaction. In contrast to S_N2 reactions for which such behavior has been experimentally documented, in the cobalt(I) reactions the metal center is the nucleophile, while the incipient ligand is the electrophile. Alternatively, these reactions could be discussed in terms of oxidative addition. By convention, the reactions with HA yield cobalt(III) hydrides and thus may be classified logically as oxidative addition. On the other hand, the product of CO addition, a five-coordinate species,[11] is reasonably regarded as a cobalt(I) complex. The implication from Figure 12 is that these formally diverse reaction types involve common activation requirements.

An interesting secondary issue posed by this model of the cobalt(I) reactions is the timing of the binding of a trans water molecule when the stable product of the addition reaction is a six-coordinate species, e.g.

$$N\text{-}rac\text{-}CoL^+ + HA \rightarrow prim\text{-}N\text{-}rac\text{-}CoL(H)^{2+} + A^- \qquad (2R)$$

$$CoL(H)^{2+} + H_2O \rightarrow prim\text{-}N\text{-}rac\text{-}CoL(H)(H_2O)^{2+}$$

or

$$N\text{-}rac\text{-}CoL^+ + H_2O \rightarrow prim\text{-}N\text{-}rac\text{-}CoL(H_2O)^+$$

$$prim\text{-}N\text{-}rac\text{-}CoL(H_2O)^+ + HA \rightarrow sec\text{-}N\text{-}rac\text{-}CoL(H)(H_2O)^{2+} + A^- \qquad (2'R)$$

In contrast to the cobalt(II) radical reactions in which the "sixth" (water) ligand is already in place when the radical adds, when association of four-coordinate cobalt(I) with CO_2, etc. is the rate-determining step, then binding of a solvent molecule to yield the six-coordinate species must follow this step. Conversely, dissociation of the CO_2 (reverse reaction in eq 10) must occur via the five-coordinate species. For the *prim-N-rac*-$CoL(CO_2)^+$ system, our failure to detect this interconversion in our highest concentration (i.e., fastest) experiments places this interconversion on the time scale of 2 μs or less. Of some relevance here is the observation that the positions trans to the methyl group in $CoL(H_2O)(CH_3)^{2+}$ are unusually labile for a cobalt(III) center; the rate constants for anation of $CoL(H_2O)(CH_3)^{2+}$ by SCN^- are as follows:[25] 5 M^{-1} s^{-1} (*prim-N-rac*-CH_3), 11 M^{-1} s^{-1} (*N*-meso), and $>1 \times 10^4$ M^{-1} s^{-1} (*sec-N-rac*-CH_3).

As noted earlier, there is some evidence that boric acid yields mixtures of primary and secondary hydrides; this suggests that eqs 2R and 2'R have comparable rates when boric acid is the proton source HA. It is conceivable that H_2O = HA reacts exclusively at the secondary face because $CoL(H_2O)^+$ is more reactive than CoL^+ in this thermodynamically uphill proton transfer. (Note that protonation of five-coordinate cobalt(I) is expected to be more thermodynamically favorable if the hydride complex is six-coordinate).

Cobalt(II) Radical Reactions. The rate constants for radical additions to CoL^{2+} in Table II depend upon both the nature of the radical and the isomer. For the *N*-meso isomer and several other cobalt(II) macrocycles, primary radical addition rate constants have been reported to be insensitive to the nature of the radical.[24] However, when the present data for H atom addition and *tert*-butyl alcohol radical addition are included in the comparison, it becomes evident that steric bulk is a factor in the additions for the *N*-meso isomer: Thus, H, CH_3, and *tert*-butyl alcohol radical rate constants are in the ratio 65/12/1 at 25 °C. Indeed, it seems reasonable that the axial methyl group on either face of the *N*-meso isomer should exert a significant steric effect with an alkyl group as bulky as the *tert*-butyl alcohol radical. While the rate constants for radical addition to CoL^{2+} are very large and quite similar for the two isomers with R = H, the *N-rac*-CoL^{2+} rate constants otherwise exhibit greater sensitivity to the steric bulk of the entering radical than does the *N*-meso isomer: For the formate radical ion, $k_M/k_R = 2.8$, for R = CH_3, $k_M/k_R = 3.8$, and for the *tert*-butyl alcohol radical, $k_M/k_R = 14$. The similarities of the rate constants for hydrogen atom addition taken with their increasing sensitivity with steric bulk of the carbon radicals suggests that both isomers may be five-coordinate, with radical addition occurring at the open site trans to bound water. For the *N*-rac isomer, this face is blocked by two axial methyl groups, while the *N*-meso isomer can only be blocked by one axial methyl. Hence, we have the greater sensitivity of the *N*-rac rate constants to the nature of the radical. Our data for methyl and *tert*-butyl alcohol radicals may also be compared with those reported by Elroi and Meyerstein[30] for other alcohol radicals reacting with *N-rac*-CoL^{2+}: $^{\bullet}CH_3$, 6×10^7 M^{-1} s^{-1}; $^{\bullet}CH_2OH$, 7×10^7 M^{-1} s^{-1}; $^{\bullet}C(CH_3)(H)OH$, 3×10^7 M^{-1} s^{-1}; $(^{\bullet}CH_2)(CH_3)_2COH$ 1.4×10^6 M^{-1} s^{-1}. Interestingly, the relative rates parallel those reported by Buxton and Green[31] for Cu^{2+}_{aq} radical additions.

As noted earlier, reaction of *N-meso*-CoL^{2+} with formate radical ion does not yield addition exclusively but rather also produces some CoL^+. The latter (plus CO_2) are the expected products for outer-sphere electron transfer to the metal center; indeed, cobalt(I) and CO_2 are the exclusive products with more readily reduced cobalt(II) complexes.[15] The yield of cobalt(I) observed here is, however, much larger than expected[32,33] for an outer-sphere electron-transfer process. We speculate that an inner-sphere pathway, involving binding of the oxygen on $^{\bullet}CO_2^-$ to the cobalt, is responsible for formation of the cobalt(I); the O-bonded CoOCO complex resulting from this inner-sphere electron transfer should be extremely unstable and dissociate rapidly to the free CoL^+ and CO_2 products.

Addition of $^{\bullet}CO_2^-$ to other transition-metal centers also yields MCO_2 complexes.[34-39] The most extensively characterized of these are formed from iron(II) aminocarboxylate complexes Fe(NTA) (NTA = nitrilotriacetate) and Fe(HEDTA) (EDTA = ethylenediaminetetraacetate) for which the formate radical addition rate constants are 1×10^7 and 6.2×10^6 M^{-1} s^{-1}, respectively, at 25 °C.[38] For these, the reverse rate constants 140 and 25 s^{-1}, respectively, could be measured, and thus the equilibrium constants (for binding of $^{\bullet}CO_2^-$) 7.1×10^4 and 2.5×10^5 M^{-1}, respectively, could be calculated. It is of some interest to

$$^{\bullet}CO_2^- + CoL^{2+} \rightleftharpoons CoL(CO_2)^+ \qquad (12)$$

evaluate the comparable equilibrium constant (K_{12}) for the present macrocyclic cobalt systems. We calculate K_{12} from K_{17} and K_{10},

(28) Edidin, R. T.; Sulivan, J. M.; Norton, J. R. *J. Am. Chem. Soc.* **1987**, *109*, 3945.
(29) Gandler, J. R.; Bernasconi, C. F. *Organometallics* **1989**, *8*, 2282–2284.
(30) Elroi, H.; Meyerstein, D. *J. Am. Chem. Soc.* **1978**, *100*, 5540.
(31) Buxton, G. V.; Green, J. C. *J. Chem. Soc., Faraday Trans. 1* **1978**, *74*, 697.
(32) Schwarz, H. A.; Creutz, C.; Sutin, N. *Inorg. Chem.* **1985**, *24*, 433.
(33) Venturi, M.; Mulazzani, Q. G.; D'Angelantonio, M.; Ciano, M.; Hoffman, M. Z. To be published, 1990.
(34) Ellis, J. D.; Green, M.; Sykes, A. G.; Buxton, G. V.; Sellers, R. M. *J. Chem. Soc., Dalton Trans.* **1973**, 1724.
(35) Kelm, M.; Lilie, J.; Henglein, A.; Janata, E. *J. Phys. Chem.* **1974**, *78*, 882.
(36) Buxton, G. V.; Sellers, R. M. *Coord. Chem. Rev.* **1977**, *22*, 195.
(37) Micic, O. I.; Nenadovic, M. T. *J. Chem. Soc., Dalton Trans.* **1979**, 2011.
(38) Goldstein, S.; Czapski, G.; Cohen, H.; Meyerstein, D. *J. Am. Chem. Soc.* **1988**, *110*, 3903.
(39) Meyerstein, D.; Schwarz, H. A. *J. Chem. Soc., Faraday Trans. 1* **1989**, *84*, 2933.

Scheme II

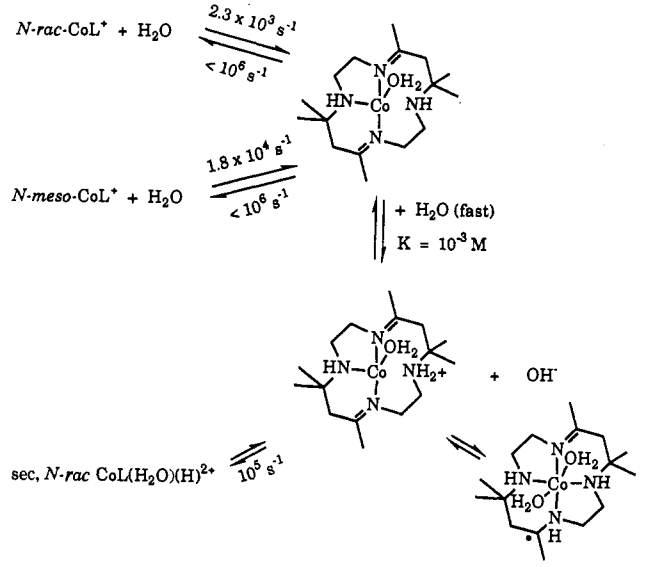

with K_{17} being evaluated from the $CO_2/{}^{\bullet}CO_2^-$ reduction potential (−1.90 V vs SHE[20]) and the $CoL^{2+/+}$ reduction potential (estimated to be −1.32 V vs SHE in water[7]). Thus, at 25 °C, the values $K_{12R} = 3 \times 10^{19}$ M^{-1} and $K_{12M} = 0.4 \times 10^{17}$ M^{-1} are obtained, and the rate constant for ${}^{\bullet}CO_2^-$ dissociation from *N-meso*-$CoL(CO_2)^+$ ($k_{-12M} = 6 \times 10^{-8}$ s^{-1}) is calculated from K_{12M} and k_{12M}.

$$ {}^{\bullet}CO_2^- + CoL^{2+} \rightleftharpoons CoL^+ + CO_2 \qquad (17) $$

"Water" Reaction. The most poorly understood aspect of these systems is the nature of the processes that limit the lifetimes of the two CoL^+ isomers in water to less than 1 ms. While *N-rac*-CoL^+ and *N-meso*-CoL^+ do interconvert slowly to give an equilibrium mixture in acetonitrile solvent,[7] the overall lifetime of CoL^+ (with very pure solvent, several weeks) is at least a factor of 10^9 longer than in water. This observation, along with the pH dependence of the phenomenon in aqueous media, implicates an acid/base role for water, and of course water may also serve as a ligand. As noted earlier, the spectra (Figure 4) determined following the decay of *N-rac*-CoL^+ implicate the production of *sec-N-rac*-$CoL(H)(H_2O)^{2+}$ and an additional species X_{500}, absorbing at longer wavelengths than the hydride. At longer times (>1 s), the conversion of X_{500} to *sec-N-rac*-$CoL(H)(H_2O)^{2+}$ is inferred. The more rapid decay of *N-meso*-CoL^+ generates similar, possibly identical, products.

If the products of *N-meso*-CoL^+ decay are indeed the same as those from *N-rac*-CoL^+ decay, then since the amine nitrogens are the chiral centers the first step is most likely the breaking of a cobalt–nitrogen (amine) bond with binding of a water molecule to the cobalt in an equatorial position. Conversion to this tridentate form is assumed to be the rate-limiting step in the decays, and the rate constant is then 2.3×10^3 s^{-1} for *N-rac*-CoL^+ and 1.8×10^4 s^{-1} for *N-meso*-CoL^+. Rapid protonation of the free amine nitrogen by water prevents reformation of the Co–N bond, thereby destroying the chiral center. Subsequent proton transfer from the amine to the cobalt yields a hydride; proton transfer to the imine, along with the electron transfer from the cobalt, yields a ligand radical species (X_{500}). If the protonation of the cobalt is assisted by the prior binding of an axial water molecule (the cobalt(III) product is six-coordinate), then the steric effects of this water would force the *N*-rac configuration with the water on the primary face. Thus, protonation would lead to the secondary hydride. This mechanism is summarized in Scheme II.

This mechanism is consistent with what is known about the likely kinetics of the various steps: The stability constants of cobalt(II) and nickel(II) polyamines increase by a factor of about 10^3 for each M(II)–N bond, and so it is reasonable that the stability constant for a cobalt(I)–amine bond should be smaller than 10^3. Thus, if the forward (bond-breaking) rate constant is 2.3×10^3 s^{-1} (*N*-rac), the reverse rate constant is 10^6 s^{-1} or less.

Table VI. Relative Stabilities of Isomers in Water at 25 °C

reaction	$K_{M,R}$
N-meso-CoL^{2+} ⇌ *N-rac*-CoL^{2+}	≥10[a]
N-meso-CoL^+ ⇌ *N-rac*-CoL^+	≥10
N-meso-$CoL(CO_2)^+$ ⇌ *prim-N-rac*-$CoL(CO_2)^+$	≥750[b]
sec-N-rac-$CoL(CO_2)^+$ ⇌ *prim-N-rac*-$CoL(CO_2)^+$	ca. 5[c]
N-meso-$CoL(CO)^+$ ⇌ *prim-N-rac*-$CoL(CO)^+$	≥20[b]
N-meso-$CoL(H)^{2+}$ ⇌ *prim-N-rac*-$CoL(H)^{2+}$	5×10^{-3}
sec-N-rac-$CoL(H)^{2+}$ ⇌ *prim-N-rac*-$CoL(H)^{2+}$	1
N-meso-$CoL(CH_3)^{2+}$ ⇌ *prim-N-rac*-$CoL(CH_3)^{2+}$	5[d]

[a] Szalda, D. J.; Schwarz, C. L.; Endicott, J. F.; Fujita, E.; Creutz, C. *Inorg. Chem.* **1989**, *28*, 3214–19. [b] Based on $K_{M,R}(Co(I)) = [N\text{-}rac\text{-}CoL^+]/[N\text{-}meso\text{-}CoL^+] \geq 10$. [c] Estimated from the magnitude of k_{-10} and dependence of other rate constants on K_{eq}. [d] Endicott, J. F.; Kumar, K.; Schwarz, C. L.; Perkovic, M. W.; Lin, W.-K. *J. Am. Chem. Soc.* **1989**, *111*, 7411.

Protonation of the free amine should be faster, about 10^7 s^{-1} if the pK_a of the free amine is 11 (i.e., $pK_{OH} \sim 3$; reverse rate constant 10^{10} M^{-1} s^{-1}). Thus, the lifetime of the protonated amine species should be longer than 10^{-4} s at pH 9, which is sufficient time for intramolecular proton transfer to the cobalt: Since the rate constant for bimolecular protonation of the cobalt by an acid with $pK_a = 11$ would be ca 10^4 M^{-1} s^{-1} and the equivalent concentration of the $-NH_2^+$ group in the complex is about 10 M, the proton transfer should occur with an intramolecular rate constant of about 10^5 s^{-1}.

The similarity of *N*-meso and *N*-rac products in Figure 4 could be just a coincidence, and the reaction could proceed by another mechanism, for instance, direct protonation of the imine nitrogen. However, the formation of the secondary hydride from *N-rac*-CoL^+ strongly suggests that a water ligand is added to the primary face of the complex prior to protonation of the metal.

Thermodynamics of Ligand Binding. Earlier work revealed that the affinities of tetraazacobalt(I) macrocycles for both CO[7] and CO_2[7,10] (and probably H^+[15], as well) increases as the $Co^{II/I}$ reduction potentials become more negative. Our studies of eq 5 indicated that the $Co^{II/I}$ reduction potentials of the *N*-meso and *N*-rac isomers are identical (c.f. the studies in acetonitrile[10]), yet their absolute and relative affinities for the three ligands studied here varies widely (Table IV): Relative to CO, the binding constants ($H^+/CO/CO_2$) are in the ratio 500/1/3 for the prim-*N*-rac complexes and >10^6/1/0.08 for the *N*-meso complexes. The CO binding constants are rather similar to one another and similar to that determined in acetonitrile;[7] by contrast, the CO_2 binding constants are much greater in water, perhaps indicating that water more effectively stabilizes the development of charge separation within the complex and also stabilizes the bound carboxylate through hydrogen bonding to the oxygen atom(s).

The relative stabilities ($K_{M,R}$) of the various isomers of the CO_2, CO, and hydride complexes studied here are summarized in Table VI, along with data for the parent cobalt(I) and cobalt(II)[12] complexes and for the methyl cobalt(III) complexes[25] from the literature. Endicott and co-workers have concluded[25] that the relative stabilities of isomers of trans disubstituted cobalt(III) complexes of L depend upon the symmetry of the complex: Symmetric substitution (diaquo, dichloro) favors the *N*-meso isomer, but asymmetric substitution favors the *N*-rac isomer in which the bulkier ligand occupies the primary face. The calculated differences between *prim-N-rac*-CH_3, the *N-meso*-, and *sec-N-rac*-CH_3 $CoL(CH_3)(H_2O)^{2+}$ complexes are 1.6 kcal mol^{-1} each, with the *prim*-CH_3 the most stable and the sec-CH_3 the least stable; the observed $K_{M,R}$ value is 5. These conclusions are generally in accord with our findings, with noteworthy exceptions to be discussed further on. The stability order predicted and observed for the methyl complexes is the same as that found for the CO_2 complexes: The *prim*-CO_2 isomer is more stable than the sec or the *N*-meso isomer, with $K_{M,R} \geq 750$ in water (in acetonitrile solvent,[7] $K_{M,R} = 2 \times 10^3$ at 25 °C, and the discrimination appears similar in DMSO[10]). For the sterically undemanding CO ligand, the stabilities of the prim and *N*-meso isomers differ less than for the CO_2 complexes. For the CO_2 complexes, both steric and possible hydrogen-bonding interactions between

the amine NH protons and bound CO_2 have been considered[7,10] as the origin of the high discrimination observed between *N-rac*-CoL^+ and *N-meso*-CoL^+. Of course, an additional factor for the six-coordinate complexes is the nature of the sixth ligand; water and acetonitrile are compact and electronically equivalent ligands (for this metal center), but other solvents or other potential ligands might increase or diminish the relative stability of the prim-*N*-rac isomer of the CO_2 complex by destabilizing or stabilizing, respectively, the six-coordinate *N-meso*-CO_2 complex. More difficult to assess, but possibly of considerable importance, is stabilization due to selective solvation of the macrocycle in the various isomers.

The stability order found for the hydride complexes (*N*-meso $\gg$ prim-*N*-rac $\approx$ sec-*N*-rac) is exceptional and surprising.[40] The *N*-meso hydride complex is evidently favored over the other two isomers by at least 3 kcal mol^{-1}. Consideration of steric interactions of the axial ligands with the macrocycle would seem to favor locating the hydride in the secondary position of the *N*-rac form of the complex. The latter would also maximize solvation of the axial water molecule bound on the primary face. The fact that the *N*-meso isomer is favored at equilibrium would then seem to require specific solvational requirements for the hydride ligand itself. At this point, any further discussion of this rather remarkable result does not seem worthwhile. However, the result does serve to teach us how subtle the effects on the binding of the axial ligands can be.[41]

Concluding Remarks. CO rapidly adds to both *N-meso-* and *N-rac*-CoL^+ to form a highly stable five-coordinate complex whose stability is relatively independent of isomer and solvent. Very rapid addition of CO_2 to *N-rac*-CoL^+ yields a strongly bound five-coordinate species at higher temperatures, but the dominant form of the complex at lower temperatures is six-coordinate. Evidently, the other two CO_2 adduct isomers and all three of the hydride complexes are six-coordinate over the accessible temperature range. These are usefully regarded as six-coordinate cobalt(III) complexes of the very high field ligands CO_2^{2-} and H^-, respectively. Despite the high affinity of CoL^+ for both CO_2 and CO, hydrides are favored below pH 3-7 (depending upon the isomer and the ligand); equilibration among CO_2, CO, and hydride complexes of a given isomer proceeds exclusively via formation of the free cobalt(I) complex. The *N*-meso hydride ($pK_a \geq 13.9$) is the thermodynamic sink of these systems, but pathways for its formation from the *N*-rac isomers are not readily accessible in acid solutions.

Acknowledgment. We thank Drs. J. Endicott and C. Schwarz for helpful discussions. This work was carried out at Brookhaven National Laboratory under Contract DE-AC02-76CH00016 with the U.S. Department of Energy and supported by its Division of Chemical Sciences, Office of Basic Energy Sciences.

(40) Mechanistic studies of the conversion of the hydroxymethyl complex *N-meso*-$CoL(CH_2OH)^{2+}$ to formaldehyde, dihydrogen and *N-meso*-CoL^{2+} confirm the high pK_a of *N-meso*-$CoL(H)^{2+}$ (Chou, M. H.; Creutz, C. Work in progress).

(41) Actually, the fact that the *N*-rac form is favored for CoL^{2+}, NiL^{2+}, and CoL^+ is equally inexplicable.

Homogeneous Catalysts for Selective Molecular Oxygen Driven Oxidative Decarboxylations

Dennis P. Riley,* Donald L. Fields, and Willie Rivers

Contribution from the Monsanto Company, 800 North Lindbergh Boulevard, St. Louis, Missouri 63167. *Received September 21, 1990*

Abstract: Cobalt(II) ion has been found to catalyze the molecular oxygen driven oxidation of *N*-(phosphonomethyl)iminodiacetic acid (PMIDA) to *N*-(phosphonomethyl)glycine (PMG) in aqueous solution.[1] This homogeneous catalytic conversion is novel and represents, in effect, an oxidative dealkylation of one carboxymethyl moiety yielding the N-substituted glycine. The reaction is selective to the desired product PMG when carried out at the natural pH of the free acid substrate ($\sim$1-2) and when carried out at substrate loadings less than 5% by weight. In addition, the catalytic system is selective for the PMIDA substrate; i.e., other closely related ligands show no reactivity, e.g., NTA, EDTA, etc. The results of kinetic and mechanistic studies on dilute systems are presented and discussed with special emphasis on how an understanding of the mechanism can make it possible to generate a catalyst system that gives high yields even with high substrate loadings. The reactions are first-order in substrate and $[Co]_t$. The oxygen pressure dependence exhibits saturation kinetics, while the selectivity increases as oxygen pressure increases. The rate is also inversely proportional to $[H^+]$. The high selectivity of the oxidation and the unique selectivity of the cobalt catalytic system for the PMIDA substrate are discussed in terms of the magnitude of the metal ligand binding constant at the low pH of the reaction.

Introduction

The ability to utilize molecular oxygen as a selective oxidizing agent has many obvious advantages owing to its abundance and low cost. An area that is of considerable continuing interest has been the oxidative dealkylation of tertiary amines to yield secondary amines.[2-7] This is of interest both for the synthetic utility[2-7] and for understanding the mechanism of biological oxidative dealkylations catalyzed by cytochrome P450 monooxygenases.[8] While there have been many reports of such studies in the literature with a variety of stoichiometric reagents, only two examples utilizing molecular oxygen in a catalyzed reaction have been described,[9,10] and these reports are for simple unfunctionalized trialkyl-substituted amines.

(1) a) Presented in part by Riley; D. P. Symposium on Atom Transfer Chemistry. 197th National Meeting of the American Chemical Society, Dallas, TX, April 10, 1989. b) Riley, D. P.; Rivers, W. U.S. Patent 4853159.
(2) Galliani, G.; Rindove, G. B. J. *Chem. Soc.*, Perkin *Trans.* 1 **1980**, 828.
(3) Burrows, E. P.; Rosenblatt, D. H. *J. Org. Chem.* **1983**, *48*, 992.
(4) Smith, J. R. L.; Mead, L. A. V. *J. Chem. Soc., Perkin Trans. 2* **1973**, 206.
(5) Hull, L. A.; Davis, G. T.; Rosenblatt, D. H. *J. Am. Chem. Soc.* **1969**, *91*, 6247.
(6) Smith, J. R. L.; Sadd, J. S. *J. Chem. Soc., Perkin Trans. 2* **1976**, 741.
(7) Day, M.; Hajela, S.; Hardcastle, K. I.; McPhillips, T.; Rosenberg, E.; Botta, M.; Gobetto, R.; LMilone, L.; Osella, D.; Belbert, R. W. *Organometallics* **1990**, *9*, 913.
(8) Smith, J. R. L.; Mortimer, D. N. *J. Chem. Soc., Chem. Commun.* **1985**, 64.
(9) Riley, D. P. *J. Chem. Soc., Chem. Commun.* **1983**, 1530.
(10) Correa, P. E.; Riley, D. P. U.S. Pat. 4565891.

0002-7863/91/1513-3371$02.50/0